2023 62nd IEEE Conference on Decision and Control (CDC)
December 13-15, 2023. Marina Bay Sands, Singapore

Impact of Misperception on Emergence of Risk in Platoon of Autonomous Vehicles

Arash Amini, Guangyi Liu, Vivek Pandey and Nader Motee

Abstract— **With the advent of advanced perception algorithms, achieving long-term autonomy in vehicle platooning has become a possibility. In this paper, we propose a framework to evaluate the risk of misperception resulting from noisy observations from the environment. Each vehicle relies on a perception unit to understand its surroundings and estimate the positions and velocities of other vehicles. We employ the Expected Shortfall (Average Value-at-Risk) measure to evaluate the risk of collision between pairs of vehicles and the risk of violating traffic laws for each vehicle under possible misperceptions. Obtaining an explicit expression for the risk measure allows us to investigate potential trade-offs between overall misperception-induced risks and network architecture. Using our framework, we demonstrate how misperception of highway traffic signs can cause phenomena similar to tailgating and quantify its impact on the risk of such events. Our results can also be used to identify vehicles that are highly susceptible to misperception and to enhance the platoon's robustness concerning overall risk measures in the presence of misperception. We validate our theoretical findings through extensive simulations.**

I. Introduction

The recent advancements in perception algorithms allow autonomous vehicles to rely more on perception sensors such as radar, sonar sensors, 2D/3D lidar and visual systems to understand the environment and other agents [7, 23, 20]. No matter how well-trained and robust perception units are designed, the observation from the environment could be disturbed or damaged. Different environmental elements such as rain or fog can significantly impair the visual sensors and make them unreliable[1, 13, 15, 4]. Therefore misperception of the environment and other cars is inevitable.

When uncertainties are introduced to a model, systematic risk measures have proven to be one of the most reliable methods to study the system's safety. Measurements such as Value-at-risk (VaR) and Expected Shortfall (Average Value-at-risk (AVaR)) which have been previously developed to study financial models [2, 16], have gained popularity in studying the risk of events in dynamical network systems [3, 21]. VaR has been successfully employed to study problems such as vehicle platooning [21, 11, 10], power network synchronizing[22], and rendezvous problems for a team of robots [12]. It is shown that not only can this framework be used to study a single event such as collision, but it is also a strong tool when cascades of events are involved.

This work was supported partly by the ONR N00014-19-1-2478 and ONR N00014-23-1-2779.

A. Amini, G.Liu, V.Pandey, and N. Motee are with the Department of Mechanical Engineering and Mechanics, Lehigh University, Bethlehem, PA 18015, USA (a.amini,gliu,vkp219,motee)@lehigh.edu

The emergence of advancements in perception algorithms [18, 19], allowed autonomous vehicles to rely on their observation of the environment rather than depending solely on communication channels. Relying on the perception unit benefits the platoon in two folds. First, it allows us to remove the communication unit, which is vulnerable with respect to adversarial attacks and failures. Additionally, communication devices are expensive and may not operate consistently across different brands of vehicles. On the other hand, with recent advancements in visual perception algorithms[9], almost all cars are equipped with cameras that allow them to perceive the environments for safety measures and collision avoidance. Like any other sensor, the perception unit is weak to input disturbances. This motivated us to design control algorithms to improve the overall robustness and performance of the systems when perception noise and ambiguities are present[8, 14].

In this paper, we consider two scenarios. First, we study the risk stemming from misperception of other vehicles' states. This scenario is similar to the case when a driver fails to estimate the other vehicle's state with accuracy. As a result, there is a large potential for increased inter-vehicle collision risk. In the second scenario, we investigate the case where the perception unit fails to perceive the traffic signs. This type of misperception is expected to happen rarely. However, the result could be fatal and extremely expensive. For instance, misperceiving a 45 mph speed sign with 65 mph will make the affected vehicle similar to an aggressive driver, which results in phenomena similar to tailgating. In both scenarios, we are not limiting our study to the risk of inter-vehicle collision and further investigating the risks induced by violating posted traffic signs, a.k.a; violation risks.

Contribution: Building upon our recent works [21, 11, 12, 14], we extend our result to the fleet of autonomous vehicles that rely on perception unit to coordinate their movements. We introduce a renewed definition for the safe sets, which allows us to extend our framework to investigate the Average Value-at-Risk for inter-vehicle collision and violation of the speed limits. We prove that the renewed risk measure enjoys properties such as *convexity*, *monotoncity* and *sub-additivity*. We further investigate how network architecture affects the risks induced by misperception and draw the fundamental inherent risk of misperception in autonomous vehicle platooning.

Mathematical Notations: We follow the traditional notation for real-valued scalars, vectors, and matrices. The set of real numbers is denoted by $\mathbb{R}$. The non-negative and positive scalars are represented by $\mathbb{R}_+$ and $\mathbb{R}_{++}$ respectively.

979-8-3503-0123-6/23/$31.00 ©2023 IEEE

We denote the vector of all ones by $\mathbf{1}_d \in \mathbb{R}^d$, the d dimensional identity matrix by $I_d \in \mathbb{R}^{d\times d}$ and matrix of all zeros by $\mathbf{0}_d \in \mathbb{R}^{d\times d}$. We represent the set of d-dimensional positive(semi)-definite matrices by $\mathbb{S}^d_{++}$ ($\mathbb{S}^d_{+}$). For a given set $\mathcal{H}$, we represent the cardinality of the set by $|\mathcal{H}|$, which measures the number of distinct elements of set $\mathcal{H}$. We employ operator ; to concatenate two column vectors $x, y \in \mathbb{R}^d$ to obtain column vector $[x; y] \in \mathbb{R}^{2d}$.

Algebraic Graph Theory: We let $\mathcal{G}$ be the undirected graph defined by $\mathcal{G} := (\mathcal{V}, \mathcal{E})$, where $\mathcal{V}$ is the set of vertices, $\mathcal{E}$ is the set of all edges. Throughout this paper we assume that the the graph $\mathcal{G}$ has n vertices, $|\mathcal{V}| = n$, and $n_{\mathcal{E}}$ edges, $|\mathcal{E}| = n_{\mathcal{E}}$. Let us define the Laplacian matrix L by

$$\begin{cases} l_{ij} = -\omega_{ij} & \text{for} \quad i \neq j \\ l_{ii} = \sum_{j=1}^{n} \omega_{ij} \end{cases}, \tag{1}$$

where ω_{ij} is the weights assigned to the edge (i, j). For undirected graphs $\omega_{ij} = \omega_{ji}$ therefore the Laplacian matrix, L, is symmetric and positive semi-definite [6]. We denote the eigenvalues of matrix L by $0 = \lambda_1 \leq \lambda_2 \leq \cdots \leq \lambda_n$, and their corresponding normalized eigenvector by q_i. We let matrix $Q = [q_1 \,|\, q_2 \,|\cdots|q_n]$ and $\Lambda = \operatorname{diag}(0, \lambda_2, \cdots, \lambda_n)$. Because the eigenvectors are normalized, Q is an orthogonal matrix, i.e., $QQ^T = Q^TQ = I_n$ and $q_1 = \frac{1}{\sqrt{n}}\mathbf{1}_n$. We let $\mathcal{N}_i$ and $D_i := \sum_{j=1}^{n} \omega_{ij}$ as the set of all neighbors and degree of agent i respectively. The diameter of the graph, denoted by $D_{\mathcal{G}}$ is defined by the longest shortest path between all pairs $(i, j) \in \mathcal{V} \times \mathcal{V}$. We denote the incident matrix of graph $\mathcal{G}$ by matrix $B \in \mathbb{R}^{n\times|\mathcal{V}|}$.

Probability Theory: A random vector $x \in \mathbb{R}^d$ is a vector of random variables. The random vector y with normal distribution which has expected values $\mu \in \mathbb{R}^d$ and Covariance matrix $\Sigma \in \mathbb{R}^{d\times d}$, is denoted by $y \sim \mathcal{N}(\mu, \Sigma)$. The error function by erf : $\mathbb{R} \to (-1, 1)$ defined by $\operatorname{erf}(x) := \frac{2}{\pi}\int_0^x e^{-t^2} dt$. The expected value of the random vector y is denoted by $\mathbb{E}[y]$.

II. Problem Statement

Let us consider a fleet of n autonomous vehicles traveling on a highway. The agents are labeled in descending order such that the n^{th} agent is considered the leader of the platoon. Each vehicle is equipped with perception sensors that allow it to observe the environment and other vehicles. We assume that each vehicle can instantly measure the distance and velocity of the observed vehicles through the perception unit. It is further assumed that each vehicle can provide a confidence score for its observations, i.e., the more accurately it can observe other vehicles and measure their states, the higher the confidence it has in its observation. In addition, the perception unit is responsible for identifying and reporting the traffic signs, such as speed limits. The vehicle controller unit uses the target velocity from the perception unit to control the vehicle's speed.

A stochastic differential equation (SDE) governs the dynamics of each agent in the network, i.e., the dynamic of i'th agent is given by

$$\begin{aligned} dx_t^{(i)} &= v_t^{(i)} dt \\ dv_t^{(i)} &= u_t^{(i)} dt + g d\xi_t^{(i)} \end{aligned} \tag{2}$$

where $x_t^{(i)} \in \mathbb{R}$, $v_t^{(i)} \in \mathbb{R}$ and $\xi_t^{(i)} \in \mathbb{R}$ are position, velocity and the exogenous disturbance of ith agent. The exogenous disturbance, $\xi_t^{(i)}$, is modeled by Brownian motion, i.e.,

$$\mathbb{E}[\xi_t^{(i)}] = 0, \qquad \mathbb{E}[\xi_t^{(i)}\xi_\tau^{(i)}] = t - \tau, \tag{3}$$

for $0 \leq \tau \leq t$. Design of control input $u_t^{(i)}$ aims to achieve three goals:

1) *Maintain* the inter-vehicle distances between the at d.
2) Agents velocities reach *consensus*.
3) Ensure that the agents follow the *traffic signs* to avoid possible penalties.

To achieve the first two objectives following the control policy was suggested by [21]

$$\begin{aligned} \hat{u}_t^{(i)} := &\sum_{j=1}^{n} \omega_{ij}\Big(v_t^{(j)} - v_t^{(i)}\Big) \\ &+ \beta \sum_{j=1}^{n} \omega_{ij}\Big(x_t^{(j)} - x_t^{(i)} - (j - i)d\Big), \end{aligned} \tag{4}$$

where $\beta \in \mathbb{R}_{++}$ is the tuning parameter to balance between the consensus of the velocities and distances. In order to achieve the third objective, we propose an updated version of the control policy (4). The modified policy is given by

$$u_t^{(i)} := \underbrace{\gamma\Big(\bar{v}_t^{(i)} - v_t^{(i)}\Big)}_{\text{Target Velocity tracking}} + \hat{u}_t^{(i)}, \tag{5}$$

where $\gamma \in \mathbb{R}_{++}$ is constant to adjust the vehicle's desire to follow the target velocity $\bar{v}_t^{(i)}$, which is provided through perception as a result of observing the speed signs. Perception measurement has proven to be robust and reliable. However, the perception unit relies on cameras and other sensors, where the input can become disturbed. As a result, there could be mismeasurement and misclassifications of the objects. The noise enters the system through the control input, $\hat{u}_t^{(i)}$, defined in (4). Authors in [8] showed that the perception noise could be modeled as an additive disturbance to the measurements. We model the disturbed control signal by

$$\begin{aligned} \hat{u}_t^{(i)} := &\sum_{j=1}^{n} \omega_{ij}\Big(v_t^{(j)} - v_t^{(i)} + g_v \mathfrak{x}_t^{(ij)}\Big) \\ &+ \beta \sum_{j=1}^{n} \omega_{ij}\Big(x_t^{(j)} - x_t^{(i)} - (j - i)d + g_x \mathfrak{y}_t^{(ij)}\Big), \end{aligned} \tag{6}$$

where $\mathfrak{y}_t^{(ij)}$ and $\mathfrak{x}_t^{(ij)}$ are the disturbance of the perception unit. Constants g_x, $g_v \in \mathbb{R}_{++}$ are indicators for noise amplitude on the velocities and position estimation, respectively. We assume that $\mathfrak{y}_t^{(ij)}$ and $\mathfrak{z}_t^{(ij)}$ are white noise with mean zero and covariance ς_{ij}.

During vehicle platooning, we assume that the underlying graph topology is fixed. Furthermore, agents are expected to have a certain distance from each other. In practice, the accuracy of the perception-based measures is significantly impacted by the distance between two vehicles. We aim to compensate for such distance-related errors by assuming that each vehicle has a reliable estimation of ς_{ij} based on the priory information and the underlying graph. When there is no prior information available, we assume that $\forall (i, j) \in \mathcal{V}$ the $\varsigma_{ij} = 1$. The prior data provide us with reliable information regarding the confidence of each perception unit in estimating other agents. Therefore, we will assign weights of the graph $\mathcal{G}$ based on the available information by

$$\begin{cases} \omega_{ij} = \dfrac{1}{\varsigma_{ij}} & \text{if}(i, j) \in \mathcal{V} \\ \omega_{ij} = 0 & \text{otherwise} \end{cases}. \tag{7}$$

When an agent has access to high-quality information about another agent, they are more likely to assign trust to their observations and the control law they employ. Conversely, agents with limited ability to observe and estimate the states of other agents may assign less confidence to their observations and control laws. In case when there are no prior information available, we assume that the misperception noise across the graph is uniform. The second source of ambiguity in the perception unit is the identification and classification of traffic signs. Despite the advances in training of perception models, the potential for misperceiving environmental data remains to be present, particularly when taking into account the combination of vehicle motion and the observation noise.

The *problem* is to quantify the risk of systematic events when the platoon relies on the perception unit to perceive the environment and other cars. The events we are considering are the inter-vehicle collision and violation of posted traffic signs on the highway. Removing the communication unit would make the agents interact implicitly in achieving consensus and maintaining the inter-vehicle distance. Explicit quantification of systematic risk allows us to revile the relation between the risk measures with underlying graph $\mathcal{G}$, misperception ambiguities, and exogenous noise.

In Section III we obtain the stationary distribution of the inter-vehicle distances and velocities. Section IV is designated to define the AVaR risk measure and computation of explicit expressions for both risks of collision and violation. We also discuss the inherent risks associated with misperceptions in Section IV. We present the case study for risk analysis of vehicle platooning under misperception in section V.

III. Stationary Behavior of Network

In vehicle platooning, vehicles adhere to their steady-state behavior. If a transient event occurs, they tend to return to their stationary distributions relatively fast [21]. Therefore in this paper, we concentrate on studying the risk of undesired events based on the stationary behavior of the agents. Let us define new set of coordinates $\boldsymbol{z}_t$ and $\boldsymbol{\nu}_t$ by

$$\boldsymbol{z}_t = Q^T(\boldsymbol{x}_t - \boldsymbol{y}), \text{ and } \boldsymbol{\nu}_t = Q^T \boldsymbol{v}_t, \tag{8}$$

where $\boldsymbol{y} := [d; 2d; \cdots ; nd]$ is the vector of desired inter-vehicle distances.

Lemma 1. *Let us assume that the vehicles have perceived the vector of target velocity by*

$$\bar{\boldsymbol{v}}_t = \begin{cases} 0 & t < 0 \\ \tilde{\boldsymbol{v}} & t \geq 0 \end{cases}, \tag{9}$$

and the weights of the graph $\mathcal{G}$ are assigned based on (7). One can decouple the dynamics of the platoon by

$$\begin{aligned} dz_t^{(i)} &= \nu_t^{(i)} dt \\ d\nu_t^{(i)} &= \left(-(\lambda_i + \gamma)\nu_t^{(i)} - \beta\lambda_i z_t^{(i)} + \gamma q_i^T \bar{\boldsymbol{v}} \right) dt + g_i d\mathfrak{z}^{(i)}, \end{aligned} \tag{10}$$

where $g_i^2 = g^2 + \lambda_i^2(\beta^2 g_x^2 + g_v^2)$ and is standard Brownian motion. Furthermore for all $i \in \{2, \cdots, n\}$ pairs $(z_t^{(i)}, \nu_t^{(i)})$ are independent from each other.

Lemma 1 demonstrates that we can decouple the dynamics of the system even when the measurement of inter-vehicle distances and velocities are affected by perception-induced disturbances. The vector of inter-vehicle distances $\bar{\boldsymbol{d}}$ is defined by

$$\bar{\boldsymbol{d}} = \tilde{E}^T Q \boldsymbol{z} + d\mathbf{1}_{n-1}, \tag{11}$$

where $\tilde{E} = [\tilde{\boldsymbol{e}}_1, \tilde{\boldsymbol{e}}_2, \cdots, \tilde{\boldsymbol{e}}_{n-1}]$ and $\tilde{\boldsymbol{e}}_i := \boldsymbol{e}_{i+1} - \boldsymbol{e}_i$.

Theorem 1. *Let us assume that $\tilde{\boldsymbol{v}}$ is the perceived target velocity of vehicles, and perception disturbance follows regime in (6). Then inter-vehicle distances $\bar{\boldsymbol{d}}$ reach a stationary multivariate normal distribution, i.e. ,*

$$\bar{\boldsymbol{d}} \sim \mathcal{N}(\mu_{\bar{\boldsymbol{d}}}, \Sigma_{\bar{\boldsymbol{d}}}) \tag{12}$$

where

$$\mu_{\bar{\boldsymbol{d}}} = \frac{\gamma}{\beta} \tilde{E}^T L^\dagger \tilde{\boldsymbol{v}} + d\mathbf{1}_{n-1}, \tag{13}$$

and

$$\sigma^2{}_{\bar{\boldsymbol{d}}}^{(i)} = \sum_{k=1}^n (\tilde{\boldsymbol{e}}_i^T \boldsymbol{q}_k)^2 \frac{\lambda_k^2(\beta g_x^2 + g_v^2) + g^2}{2\beta\lambda_k(\lambda_k + \gamma)}, \tag{14}$$

where $\sigma^2{}_{\bar{\boldsymbol{d}}}^{(i)}$ are the diagonal elements of matrix $\Sigma_{\bar{\boldsymbol{d}}}$. In addition, for the velocities of vehicles, it follows

$$\boldsymbol{v} \sim \mathcal{N}\left(\frac{1}{n}\mathbf{1}_n^T \tilde{\boldsymbol{v}}, \Sigma_{\boldsymbol{v}}\right), \tag{15}$$

where

$$\sigma^2{}_{\boldsymbol{v}}^{(i)} = \sum_{k=1}^n (\boldsymbol{e}_i^T \boldsymbol{q}_k)^2 \frac{\lambda_k^2(\beta g_x^2 + g_v^2) + g^2}{2\beta\lambda_k}, \tag{16}$$

where $\sigma^2{}_{\boldsymbol{v}}^{(i)}$ are the diagonal elements of matrix $\Sigma(\boldsymbol{v})$.

Proof. Using Lemma 1 we can decouple the systems, and the decouple systems' states are independent. Combining the results of Lemma 1 and elementary linear algebra, one can prove the results. $\square$

In this paper, we want to focus our attention on the risk induced by misperceptions. In other words, when there are no exogenous disturbances applied to the vehicles, i.e., $g = 0$, and the only source of the disturbances is misunderstanding each other velocities and distances. Thus, we can further simplify the results presented in Theorem 1 by

$$\sigma^{2}{}_{\bar{\boldsymbol{d}}}^{(i)} = \sum_{k=2}^{n} (\tilde{\boldsymbol{e}}_i^T \boldsymbol{q}_k)^2 \frac{\lambda_k(\beta g_x^2 + g_v^2)}{2\beta(\lambda_k + \gamma)}, \tag{17}$$

$$\sigma^{2}{}_{\boldsymbol{v}}^{(i)} = \frac{(\beta g_x^2 + g_v^2)}{2\beta} D_i, \tag{18}$$

where D_i the degree of agent i. Theorem 1 illustrate that the misperception of posted speed signs on the highway doesn't influence the stability of the platoon. However, it's going to impact the expected inter-vehicle distance and consensus velocities.

IV. Misperception Induced Risks

In this section, we discuss the risks induced by misperception. We aim to investigate the events that interrupt vehicle platooning, such as inter-vehicle collisions and violations of traffic laws. In the latter case, even if one vehicle breaks a traffic law and law enforcement requires it to stop, the entire platooning will be impacted. From the perspective of platoon design, traffic law violations, and collisions have the same cost in terms of interrupting traffic flow. In order to incorporate the severity of the failure and utilize the properties of the risk measure, we consider the Average Value-at-Risk measure (AVaR) [5, 17]. AVaR evaluates the expected outcome of the system's state when it surpasses the Value-at-Risk (VaR). In this paper, we consider a variance of the original AVaR that is defined using the parameterized level sets U_δ, which quantifies the expected outcome, in terms of $\delta \in [0\,,1]$, when the state (or the observable) of the system is below its corresponding VaR. Let us define a family of nested sets U_δ that is parameterized by $\{\delta_k\}_{k=0}^{\infty}$ with $\lim_{k\to\infty} \delta_k = 1$. The set U_1 represents the undesired values of states, and $\mathbb{R}^n \setminus U_0$ denotes the safe state values for operation. The nested sets construct an alarm zone between U_∞ and $\mathbb{R}^n \setminus U_0$, and it satisfies following properties:

- $U_{\delta_2} \subset U_{\delta_1}$ if $\delta_1 < \delta_2$
- $\bigcap_{k=0}^{\infty} U_{\delta_k} = U_{\delta_\infty}$ with $\lim_{k\to\infty} \delta_k = 1$

The Value-at-Risk measure is then defined by

$$\mathrm{VaR}_\varepsilon(x) := \inf_\delta \left\{ \delta \geq 0 \;\middle|\; \mathbb{P}\{x \in U_\delta\} < \varepsilon \right\}, \tag{19}$$

and the corresponding AVaR is then defined by

$$\mathcal{R}_\varepsilon := \frac{1}{\varepsilon} \int_0^\varepsilon \mathrm{VaR}_\alpha \, d\alpha,$$

where $1 - \varepsilon \in (0, 1)$ denotes the confidence level.

A. Risk of Inter-Vehicle Collision

To evaluate how dangerously a pair of vehicles is close to a collision, we define the level sets

$$U_\delta = \left(-\infty, \frac{d}{c}(1 - \delta) \right).$$

The zone for potential collisions in between the agents is defined by $\bar{d}_i \in (0, d/c)$, where parameter $c \geq 1$ determines the upper end-point of the collision set U_δ. For instance, $c = 2$ means no risk is involved when the distance between the pair of agents is in $[d/2, d]$. When $c = 1$, there is no acceptable tolerance for deviations from the target distance d. The AVaR measure for collision in a platoon of the inverted pendulum is presented in the following theorem.

Theorem 2. *Let us assume that the platoon of vehicles has a stationary behavior given in Theorem 1 in the absence of exogenous disturbance, and the perceived target velocity is given by $\tilde{v}$. The risk of encountering an inter-vehicle collision for i'th pair is given by*

$$\mathcal{R}^i_{\varepsilon,C} := \begin{cases} 0, & \textit{if } \ \sigma_{\bar{d}}^{(i)} \leq \frac{1}{\kappa_\epsilon}(\mu_{\bar{d}}^{(i)} - \frac{d}{c}) \textit{ or } \varepsilon \geq \frac{1}{2} \\ 1 - \frac{c}{d}(\mu_{\bar{d}}^{(i)} - \kappa_\varepsilon \sigma_{\bar{d}}^{(i)}), & \textit{if } \ \frac{1}{\kappa_\epsilon}(\mu_{\bar{d}}^{(i)} - \frac{d}{c}) \leq \sigma_{\bar{d}}^{(i)} \leq \frac{\mu_{\bar{d}}^{(i)}}{\kappa_\varepsilon} \\ 1, & \textit{if } \ \frac{\mu_{\bar{d}}^{(i)}}{\kappa_\varepsilon} \leq \sigma_{\bar{d}}^{(i)} \end{cases},$$

where $\kappa_\varepsilon = \dfrac{e^{-\iota_\varepsilon^2}}{\varepsilon\sqrt{2\pi}}$, *given that* $\iota_\varepsilon = \mathrm{erf}^{-1}(1 - 2\varepsilon)$.

The risk measure defined in Theorem 2 deviates from the risk defined in our previous works [21, 11, 12]. The risk measure $\mathcal{R}^i_{\varepsilon,C}$ takes values from interval $[0\;,\;1]$ where one indicates maximum risk. The updated definition of level sets allows us to calculate the AVaR measure explicitly. Building upon the results of Theorem 2 one can prove that the risk measure $\mathcal{R}^i_{\varepsilon,C}$ enjoys properties such as convexity.

Corollary 1. *The risk measure $\mathcal{R}^i_{\varepsilon,C}$, defined in Theorem 2 is normalized, convex, monotone and sub-additive.*

We need to emphasize that the risk measure$\mathcal{R}^i_{\varepsilon,C}$ enjoys most of the properties of a coherence risk measure except positive homogeneity and shift invariant.

B. Risk of Violation of Speed Limits

The risk of breaking traffic laws while platooning is explored in this section when misperceptions emerge. Although violation of traffic signs seems less costly for a platoon than collision, both events would lead to disruption of the traffic flow. We need to remove vehicles from the fleet and rewire the control policy according to the new graph topology. Let us assume that the maximum and minimum allowed speed is given by v^+ and v^-, respectively. We define the violation level sets by

$$\mathcal{U}^v_\delta = \left(v^+(1 + \delta c_v), \infty \right),$$
$$\mathcal{L}^v_\delta = \left(-\infty, v^-(1 - c_v\delta) \right),$$

where $\mathcal{U}^{v^+}_\delta$ and $\mathcal{L}^{v-}_\delta$ are the corresponding unsafe level sets for maximum and minimum allowed speed and $c_v \in \mathbb{R}_{++}$. The intervals $[v^+, v^+(1 + \delta c_v)]$ and $[v^-(1 - \delta c_v), v^-]$ are the potential violation regions. Speed limit violations are inevitable. However, not all violations are treated the same. Defining the potential violation region allows us to define risk proportionally to violation cost. We define the risk of violation of the lower and upper bounds of the speed limits based on (19). The following Theorem helps us to calculate the risk of violation of speed signs explicitly.

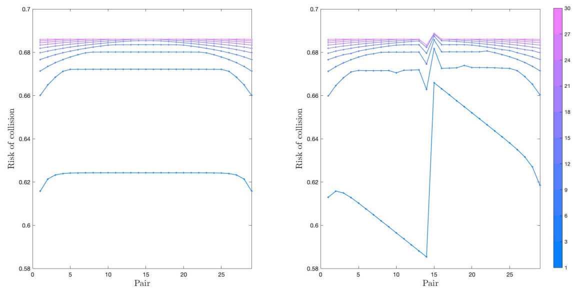

Fig. 1: Risk of collision for k-path graphs ($1 \leq k \leq 30$). Left no misperception of traffic signs, and right the middle pair misperceived.

Theorem 3. *Let us assume that the platoon of vehicles has a stationary behavior described in Theorem 1 in the absence of exogenous disturbance and the perceived target velocity is given by $\tilde{v}$. Then the risk of violation of maximum and minimum speed limit are given by*

$$\mathcal{R}^{i,\pm}_{\varepsilon,V} := \begin{cases} 0, & \text{if } \sigma_v^{(i)} \leq \frac{v^{\pm} \mp \mu_v^{(i)}}{\kappa_\epsilon} \text{ or } \varepsilon \geq \frac{1}{2} \\ \frac{\kappa_\varepsilon \sigma_v^{(i)} \pm \mu_v^{(i)}}{c_v v^{\pm}} \mp \frac{1}{c_v} & \text{if } \frac{v^{\pm} \mp \mu_v^{(i)}}{\kappa_\epsilon} \leq \sigma_v^{(i)} \leq \frac{v^{\pm}(cv \pm 1) \mp \mu_v^{(i)}}{\kappa_\epsilon} \\ 1, & \text{if } \frac{v^{\pm}(cv \pm 1) \mp \mu_v^{(i)}}{\kappa_\epsilon} \leq \sigma_v^{(i)} \end{cases}$$

where $\kappa_\varepsilon = \dfrac{e^{-\iota_\varepsilon^2}}{\sqrt{2\pi}}$, *given that* $\iota_\varepsilon = erf^{-1}(1 - 2\varepsilon)$.

Finally, we let the overall risk of violation is the maximum risk involved between the two speed limits and is given by

$$\mathcal{R}^{i}_{\varepsilon,V} = \max\{\mathcal{R}^{i,+}_{\varepsilon,V}, \mathcal{R}^{i,-}_{\varepsilon,V}\}.$$

C. Inherent Risk of Misperception

Theorem 2 and 3 provide an explicit expression for AVaR of collision and violation with respect to the graph $\mathcal{G}$. It permits us to investigate further how network architecture interplay with the risks induced by misperceptions.

Theorem 4. *Let us assume that graph $\mathcal{G}$ has diameter $D_\mathcal{G}$ and all agents perceive the traffic signs correctly. Then the inherent Average Value-at-Risk is given by*

$$\mathcal{R} = \begin{cases} 0, & \text{if } \mathcal{C}_1(D) \text{ or } \varepsilon \geq \frac{1}{2} \\ 1 - c + \dfrac{2c\kappa_\varepsilon g_p}{\sqrt{4 + \gamma n D_\mathcal{G}}} & \text{if } \mathcal{C}_2(D_\mathcal{G}) \\ 1, & \text{if } \mathcal{C}_3(D_\mathcal{G}) \end{cases}, \quad (20)$$

where $g_p^2 := \dfrac{\beta g_x^2 + g_v^2}{2\beta}$ *and* $C_\square$, $\square \in \{1,2,3\}$ *are given by*

$$\mathcal{C}_1(D_\mathcal{G}) : D_\mathcal{G} \leq \frac{1}{n\gamma}\Big[(\frac{2c\kappa_\varepsilon g_p}{c-1})^2 - 4\Big],$$

$$\mathcal{C}_2(D_\mathcal{G}) : \frac{1}{n\gamma}\Big[(\frac{2\kappa_\varepsilon g_p}{c-1})^2 - 4\Big] \leq D_\mathcal{G} \leq \frac{1}{n\gamma}\Big[(2\kappa_\varepsilon g_p)^2 - 4\Big],$$

$$\mathcal{C}_3(D_\mathcal{G}) : \frac{1}{n\gamma}\Big[(2\kappa_\varepsilon g_p)^2 - 4\Big] \leq D_\mathcal{G}.$$

Theorem 4 allows us to find a fundamental risk for collision-induced misperceptions among all possible graph

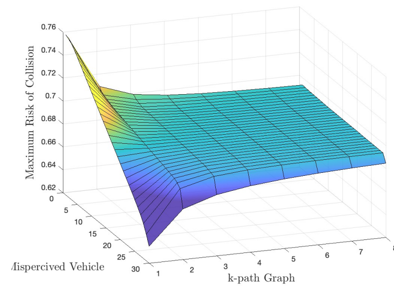

Fig. 2: Maximum collision risk for different k-path graphs when different vehicles misperceive the speed limit.

structures for a given graph diameter. Similar bounds can be derived for the risk of violation based on the fact that

$$g_p D_{\min} \leq \sigma_{\boldsymbol{v}}^{(i)} \leq g_p D_{\max},$$

where $D_{\min}$ and $D_{\max}$ are the minimum and maximum degree of the graph. The risk of violation is monotonically increasing with the degree of agent i. As a result, increasing the connectivity of an agent will result in a higher level of violation risk.

The issue of modifying the graph to minimize risks becomes more intricate when misinterpretations of traffic signs are involved. When there are possible misperceptions of traffic signs, Theorem 1 shows that the expected value of the inter-vehicle distance is modeled based on the underlying graph and position of the misperception. For instance, when a vehicle perceives a larger speed limit than reality, it starts approaching the car in front to accelerate the whole network.

V. Case Study

A platoon of 30 agents traveling on a highway with control policy (6) is considered. We investigate the risks induced by misperceptions for the path graph, k-path graph, and complete graph. k-path graph is the graph in which each agent can observe k neighbors in front and back if such neighbors exist. For all the results presented here, we set $n = 30,\ g_p = 0.3,\ \gamma = 0.2,\ \beta = 1,\ d = 1.8,\ c = 2,\ c_v = 0.1$. The confidence level, ε is set at 1 percent. The lower and upper bound for speed limits are assumed to be ± 10 percent of the true speed sign. We further assume that agents might misperceive the posted traffic signs as 10 percent more than the posted sign.

A. Complete Graph

The complete graph has a symmetric structure where $\lambda_i = \omega n$, for $i \in \{2, \cdots, n\}$ and ω is the uniform weight across the graph. It is immediate that the risk of violation is uniform across the graph and maximized compared to all other graphs. The complete graph localizes the effects of misperceptions of traffic signs. Thus, the only vehicles affected by misperceptions are the immediate neighbors. We must emphasize that the complete graph is unrealistic when relying on the perception unit, and the risk of violation are at maximum on this type of graph.

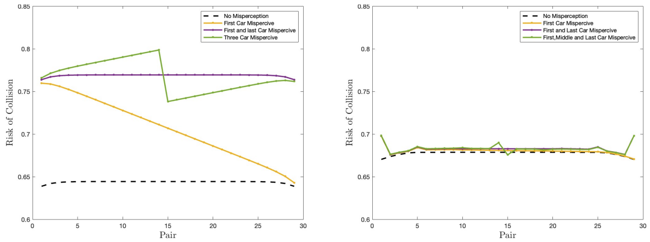

(a) Path Graph. (b) k-path Graph ($k = 4$)

Fig. 3: Risk of collision for multiple misperceptions for path and 4-path graph.

B. Path Graph

The path graph corresponds to the case where each agent can only perceive the most immediate neighbor on the fleet. Figure 1 illustrates that the path graph corresponds to the minimum collision risk in the absence of traffic sign misperception. However, when the middle pair misperceives the speed limit, the risk of collision for all other fleet members is extremely affected. In other words, the path graph is extremely vulnerable with respect to the misperception of traffic signs.

C. k-Path Graph

Figure 1 depicts the results for path graph, k-path ($k \in \{4, 7, \cdots, 28\}$) and the complete graph. The risk of collision in the absence of traffic sign misperception increases from the path graph to the complete graph when we increase k. Meanwhile, the robustness concerning misperceptions of the traffic signs significantly increases with an increase of k. When multiple vehicles misperceive the traffic signs, as illustrated in Figure 3, the path graph starts to show a significant increase in the Risk of collision. At the same time, such misperceptions have minor effects on the 4-path graph.

Figure 2 shows how the position of vehicles that misperceives the traffic sign affects the maximum risks of collision in the network with respect to different k-path graphs. It is clear that extending the capability of vehicles to perceive additional neighbor cars increases the overall network's robustness to misperceptions while keeping the risk of violations at a minimum.

VI. Conclusion

We have formulated a systematic framework to investigate the Average Value-at-Risk (AVaR) measure for a fleet of autonomous vehicles that rely on a perception unit to travel in coordination. The renewed AVaR measures enjoy properties such as convexity, sub-additivity and monotonicity which would help pave the road for solving the problem of risk minimization over the network of agents. Quantifying explicit expression for AVaR allows us to demonstrate how the misperception of other agents' states will propagate through the network. We further quantify risks induced by the misperception of traffic signs and how they interplay with the underlay graph structure.

References

[1] Arash Amini, Guangyi Liu, and Nader Motee. "Robust Learning of Recurrent Neural Networks in Presence of Exogenous Noise". In: *2021 60th IEEE Conference on Decision and Control (CDC)*. IEEE. 2021, pp. 783–788.

[2] Philippe Artzner et al. "Coherent measures of risk". In: *Mathematical finance* 9.3 (1999), pp. 203–228.

[3] Bassam Bamieh et al. "Coherence in large-scale networks: Dimension-dependent limitations of local feedback". In: *IEEE Transactions on Automatic Control* 57.9 (2012), pp. 2235–2249.

[4] Won-Seok Choi and Se-Young Oh. "Robust EKF-SLAM method against disturbance using the shifted mean based covariance inflation technique". In: *2011 IEEE International Conference on Robotics and Automation*. IEEE. 2011, pp. 4054–4059.

[5] So Yeon Chun, Alexander Shapiro, and Stan Uryasev. "Conditional value-at-risk and average value-at-risk: Estimation and asymptotics". In: *Operations Research* 60.4 (2012), pp. 739–756.

[6] Fan RK Chung. *Spectral graph theory*. Vol. 92. American Mathematical Soc., 1997.

[7] Liliaokeawawa Cothren et al. "Perception-Based Sampled-Data Optimization of Dynamical Systems". In: *arXiv preprint arXiv:2211.10020* (2022).

[8] Sarah Dean et al. "Robust guarantees for perception-based control". In: *Learning for Dynamics and Control*. PMLR. 2020, pp. 350–360.

[9] Varun Ravi Kumar et al. "Omnidet: Surround view cameras based multi-task visual perception network for autonomous driving". In: *IEEE Robotics and Automation Letters* 6.2 (2021), pp. 2830–2837.

[10] Guangyi Liu, Christoforos Somarakis, and Nader Motee. "Emergence of Cascading Risk and Role of Spatial Locations of Collisions in Time-Delayed Platoon of Vehicles". In: *2022 IEEE 61st Conference on Decision and Control (CDC)*. IEEE. 2022, pp. 6460–6465.

[11] Guangyi Liu, Christoforos Somarakis, and Nader Motee. "Risk of Cascading Failures in Time-Delayed Vehicle Platooning". In: *2021 60th IEEE Conference on Decision and Control (CDC)*. IEEE. 2021, pp. 4841–4846.

[12] Guangyi Liu et al. "Risk of Cascading Failures in Multi-agent Rendezvous with Communication Time Delay". In: *2022 American Control Conference (ACC)*. IEEE. 2022, pp. 2172–2177.

[13] Guangyi Liu et al. "Robustness analysis of classification using recurrent neural networks with perturbed sequential input". In: *arXiv preprint arXiv:2203.05403* (2022).

[14] Guangyi Liu et al. "Symbolic Perception Risk in Autonomous Driving". In: *arXiv preprint arXiv:2303.09416* (2023).

[15] Luca Mora, Xinyi Wu, and Anastasia Panori. "Mind the gap: Developments in autonomous driving research and the sustainability challenge". In: *Journal of cleaner production* 275 (2020), p. 124087.

[16] R Tyrrell Rockafellar. "Coherent approaches to risk in optimization under uncertainty". In: *OR Tools and Applications: Glimpses of Future Technologies*. Informs, 2007, pp. 38–61.

[17] R. Tyrrell Rockafellar and Stanislav Uryasev. "Conditional value-at-risk for general loss distributions". In: *Journal of Banking and Finance* 26.7 (2002), pp. 1443–1471.

[18] Francisca Rosique et al. "A systematic review of perception system and simulators for autonomous vehicles research". In: *Sensors* 19.3 (2019), p. 648.

[19] Weijing Shi et al. "Algorithm and hardware implementation for visual perception system in autonomous vehicle: A survey". In: *Integration* 59 (2017), pp. 148–156.

[20] Arien P Sligar. "Machine learning-based radar perception for autonomous vehicles using full physics simulation". In: *IEEE Access* 8 (2020), pp. 51470–51476.

[21] Christoforos Somarakis, Yaser Ghaedsharaf, and Nader Motee. "Risk of collision and detachment in vehicle platooning: Time-delay–induced limitations and tradeoffs". In: *IEEE Transactions on automatic control* 65.8 (2019), pp. 3544–3559.

[22] Christoforos Somarakis, Guangyi Liu, and Nader Motee. "Risk of Phase Incoherence in Wide Area Control of Synchronous Power Networks". In: *arXiv preprint arXiv:2112.14675* (2021).

[23] Jiachen Yang et al. "Visual perception enabled industry intelligence: state of the art, challenges and prospects". In: *IEEE Transactions on Industrial Informatics* 17.3 (2020), pp. 2204–2219.